NACA

RESEARCH MEMORANDUM

DE-ICING AND RUNBACK CHARACTERISTICS OF THREE CYCLIC

ELECTRIC, EXTERNAL DE-ICING BOOTS EMPLOYING

CHORDWISE SHEDDING

By Robert S. Ruggeri

Lewis Flight Propulsion Laboratory
Cleveland, Ohio

NATIONAL ADVISORY COMMITTEE
FOR AERONAUTICS
WASHINGTON
May 25, 1953

NATIONAL ADVISORY COMMITTEE FOR AERONAUTICS

RESEARCH MEMORANDUM

DE-ICING AND RUNBACK CHARACTERISTICS OF THREE CYCLIC, ELECTRIC,

EXTERNAL DE-ICING BOOTS EMPLOYING CHORDWISE SHEDDING

By Robert S. Ruggeri

SUMMARY

An icing investigation was conducted in the Lewis icing research
tunnel to determine the general de-icing and runback characteristics of
three production samples of electric rubber-clad cyclic de-icing boots.
The boots were all designed for the same jet airplane and, hence, were
of the same type and were designed to operate at the same values of
power density, heat-on time, and cycle ratio. The basic differences
among the various boots were in the arrangement and construction of the
heater-resistance elements. Each boot employed chordwise shedding and
contained a parting strip designed for continuous heating.

The over-all de-icing characteristics of two of the boots investi-
gated were quite similar. The de-icing protection afforded by the boot
having small unheated areas existing between segments was slightly less
than that of the other two boots. The over-all runback characteristics
of the boots were similar for the icing conditions under which the per-
formance was evaluated. The critical areas for all boots investigated
were the most forward cycled segments on the upper and lower surfaces
(located adjacent to the parting strip). While operating at design
power densities and at an angle of attack of 2°, the range of free-
stream total temperatures at which the icing protection afforded by the
various boots became marginal was from 12° to 15° F for an icing condi-
tion having a free-stream velocity of approximately 395 feet per second,
a liquid-water content of 0.5 to 0.6 gram per cubic meter, and a droplet
diameter from 12 to 14 microns.

INTRODUCTION

The NACA Lewis laboratory is currently engaged in a general inves-
tigation of cyclic de-icing of airfoils, which includes the study of
various heaters and methods of heating the surface susceptible to icing.
Cyclic de-icing of airfoils is that method of thermal ice prevention
whereby ice is allowed to form on the airfoil for a relatively short
period of time; heat is then applied at a rate sufficient to melt the
bond between the ice and the airfoil surface and allow aerodynamic

forces to remove the ice. Upon ice removal, heat is discontinued and
the surface is allowed to cool and again to accumulate ice. The cycle
is repeated at regular intervals. The principal advantage of the
cyclic system over the continuously heated system is the large saving
realized in over-all input power requirements (ref. 1).

Inasmuch as previous NACA cyclic de-icing studies (refs. 2 and 3)
have all employed models designed specifically for research purposes,
this icing investigation was conducted to determine the icing-protection
performance and runback characteristics of three samples of actual pro-
duction de-icing boots. The boots were investigated at two values of
angle of attack and free-stream velocity over a range of free-stream
total temperatures, liquid-water contents, and droplet sizes.

APPARATUS AND PROCEDURE

Three de-icing boots, which are of the same type but differ con-
siderably in construction and arrangement of heater-resistance elements,
were included in the investigation. Although the internal construction
of the various boots differs, the boots are all designed to meet the
same design and operating specifications. They are of the cyclic,
electric, rubber-clad type, and all are designed for the same fighter-
type jet airplane. Each boot is 1/8 inch thick (with 0.020-in. rubber
over the resistance elements), and each contains a parting strip
$1\frac{1}{2}$ inches wide designed for continuous operation at a power density
of 13.0 watts per square inch. The design power density for the cycled
areas of the various boots is 21.0 watts per square inch. All boots
were approximately 28 inches long (spanwise) and extended approximately
12 to 13 inches along the upper and lower surfaces of the airfoil model.
A photograph showing two de-icing boots mounted on the airfoil model
employed in the investigation is shown in figure 1. Two different boots
were mounted simultaneously on the model in order to obtain a better
comparison of the performance characteristics of the boots under identi-
cal icing conditions.

Whereas previous NACA investigations of cyclic de-icing have all
employed models using the principle of spanwise shedding, the boots
included in this investigation employed the principle of chordwise shed-
ding of ice. Chordwise shedding differs from spanwise shedding only in
the manner in which the cycled portions of the boot are divided into
segments. A sketch showing two hypothetical de-icing-boot installations
on the wing of the same fighter-type jet aircraft is shown in figure 2.
The boot shown in figure 2(a) provides spanwise shedding of ice, whereas
the boot installation shown in figure 2(b) provides chordwise shedding.

If the boots are assumed to be comparable in every respect, the
boot employing spanwise shedding might operate as follows: Heat is
first applied to cycled area 1 (upper and lower surface) for a specified
period of time. When heat is discontinued on area 1, it is immediately
applied to area 2; proceeding in a spanwise direction until all areas
have been heated. For the case of chordwise shedding (fig. 2(b)), the
boot is divided into six segments distributed three on the upper and
three on the lower surface of the airfoil. Heat might again be applied
first to area 1, then to area 2, and so forth, progressing in a chord-
wise direction across the upper surface of the airfoil and then in like
manner across the lower surface.

For purposes of identification throughout this report, the three
boots employed in the investigation are labeled A, B, and C, and the
cycled segments of each boot are labeled as shown in figure 3. The
first letter of the segment notation (A, B, or C) denotes the boot which
contains the segment; the second letter (U or L) denotes upper or lower
surface; and the number in the segment notation indicates the relative
position of the segment with respect to the parting strip. For example,
segment BU2 is the second segment of boot B aft of the parting strip
on the upper surface of the airfoil.

X-ray photographs showing the internal construction of each boot
employed in the investigation are shown in figure 4. The photographs
show a small representative area of each boot and are four-fifths scale
reproductions of the internal construction of the boots. Boot A
(fig. 4(a)) includes a parting strip and six cycled segments evenly dis-
tributed around the airfoil. Each segment is approximately $3\frac{7}{8}$ inches
wide (chordwise). The solid resistance wires of the cycled segments run
in a chordwise direction, that is, parallel to the air flow with the
boot mounted on the model. The power leads shown lie beneath the resist-
ance wires with a layer of insulation between the resistance elements
and the power leads. The heavy dark areas are bus bars to which the
resistance wires are soldered. Approximately 1/8 to 3/16 inch of unheated
area exists between the bus bars of adjacent segments of the boot.

Boot B (fig. 4(b)) also consists of a parting strip and six cycled
segments, with the segments arranged in a manner very similar to that
described for Boot A. All cycled segments are approximately 4 inches
wide, with the exception of segments BU3 and BL3, which are 3.1 inches
wide. All heater wires, however, are stranded, run in a spanwise direc-
tion, and woven into a heavy fabric. Hence, as a result of weaving,
when the fabric is sandwiched between two layers of rubber, the resist-
ance wires present a pattern similar to a shallow sine wave in a plane
perpendicular to the outer surface of the boot.

Boot C (fig. 4(c)) consists of a parting strip and eight cycled segments, arranged four segments on each side of the parting strip. The segments are approximately $3\frac{1}{8}$ inches wide in the chordwise direction, except segments CU4 and CL4, which are approximately $1\frac{1}{16}$ inches wide for the boot used in the investigation. The solid heater wires are crimped (sine-wave configuration) in a plane parallel to the outer surface of the boot to compensate for dimensional changes due to heating or flexing.

Boots A and C were cured on stainless-steel platens and, hence, possess a smooth and rather glossy surface. Boot B was cured on holland cloth, which resulted in a very fine textured cloth-like appearance of the surface.

The cycling of the boots was accomplished by means of an automatic timer designed to provide a normal cycle ratio of 10 for an individual segment of the cycled areas. The timing for a normal cycle for each segment of a boot was approximately 10-seconds heat-on, 90-seconds heat-off. This timing was changed, however, from time to time during the course of the investigation by manual switching of the timer circuit.

The cycling was identical for the three boots investigated and was done in the following prescribed manner: Cycling began with the application of heat to segment U1 (see fig. 3). The instant heat was terminated on U1, it was applied to U2, and so on, progressing in a chordwise direction across the upper surface of the airfoil. The instant heat was terminated on the most rearward segment on the upper surface, it was applied to segment L1 and progressed across the lower surface. After application of heat to the rearmost segment on the lower surface, cycling was discontinued and ice was allowed to form on the airfoil. The complete cycle was repeated at regular intervals. The parting strip was continuously heated throughout the icing investigation.

The internal circuitry of the boots was quite similar. The circuitry of each segment of each boot (including the parting strip) was arranged in a series-parallel circuit as shown by the schematic diagram presented in figure 5. For boots B and C, several sets of individual heater wires arranged in parallel were wound back and forth spanwise in each segment of the boot. At the spanwise end of each segment, the wires were fastened to electrically conductive strips. In general, the method of construction employed for boot A was similar to that employed for boots B and C, except that in this case, the sets of wires ran back and forth chordwise and were fastened to bus bars which ran in a spanwise direction (see fig. 4). The location of bus bars shown in figure 5 is representative of boots B and C. All segments of the boots were internally connected to a common ground.

2786

    The model employed in the icing investigation of the various boots
was an NACA 65-213 airfoil section having a 9.3° leading-edge sweepback,
an 82.3-inch chord at the center line, and a 71-inch total span. The
model is symmetrical about the center line and was mounted vertically
in the 6- by 9-foot test section of the icing research tunnel. The air-
foil was constructed similarly to an actual wing section of the particu-
lar fighter-type jet airplane for which the boots were designed and,
hence, incorporated taper in addition to the leading-edge sweepback. A
schematic drawing of the model employed in the investigation is shown
in figure 6.

    The boots were mounted on removable leading edges (1/8-in. aluminum
skin) to facilitate installation of the boots. Boot A, which was arbi-
trarily chosen as a standard for comparison, was mounted on the upper
half of the airfoil model (fig. 1). Boots B and C were mounted alter-
nately on the lower portion of the model. A hot-air anti-icing cuff was
provided to prevent the formation of ice on the unheated area between
the two boots.

    The instrumentation of the boots employed in the investigation was
rather limited in scope, consisting of only two thermocouples for each
segment of a boot. The surface thermocouples consisted of 30-gage iron-
constantan wire rolled into ribbons approximately 0.0025 inch thick.
The ribbons were butt-welded and laid chordwise over the surface of the
boot with the junction located at the approximate center of each segment.
Thermocouples were also installed in the aluminum skin underneath the
boot at the approximate center of the boot segments.

    The performance of the boots was studied for a constant free-stream
velocity of approximately 395 feet per second, with the exception of one
run that was conducted at a lower free-stream velocity of 288 feet per
second. The angles of attack employed were 2° and 6°. The free-stream
total temperature was varied from 0° to 25° F, and the liquid-water con-
tent from 0.20 to 1.8 grams per cubic meter.

                            RESULTS AND DISCUSSION

    The results presented herein were obtained largely from visual
observations and photographs of icing of the various boots. In certain
instances, surface-temperature data were obtained in conjunction with
the visual and photographic data. Although these temperature data are
not available for each test condition investigated, sufficient data are
available to evaluate the over-all performance characteristics of the
boots.

Boot Surface Temperatures

    Typical surface-temperature distributions measured in dry air and
in a moderate icing condition for boots A, B, and C are presented in fig-
ure 7. The curves were obtained with the boots operating on normal cycle
and at design power densities. Normal cycle indicates a heat-on time of
approximately 10 seconds and a cycle ratio of 10 for an individual cycled
segment of the boot. All temperatures presented in figure 7 are peak
temperatures measured at the instant power was discontinued on a particu-
lar segment of the boot. Surface temperature is plotted against s/c,
where s/c is the ratio of surface distance (measured from the leading
edge) to the chord length measured at the planes of instrumentation,
expressed in percent. The surface-temperature distribution obtained for
each boot operating in dry air at a free-stream total temperature of
15° F, a free-stream velocity of 396 feet per second, and an angle of
attack of 2° is presented in figure 7(a). The maximum surface tempera-
ture measured for all three boots occurred at values of s/c between
zero and 4.0 percent on the lower surface. The minimum surface tempera-
tures occurred on the upper surface of the boots. The variation in sur-
face temperature for each boot ranged from approximately 20° F for boot A
to more than 40° F for boot B.

    The variation of surface-temperature distribution measured for
boots A, B, and C in an icing condition is plotted in figure 7(b). The
data shown are for a liquid-water content of 0.57 gram per cubic meter
and a droplet diameter of 12 microns. The lowest surface temperature
measured in icing occurred at or very near the parting-strip area for
each boot. The minimum temperatures are all below 50° F, with the
parting strip of boot B reading the lowest value of approximately 43° F.
Photographs presented later in the discussion will show that the surface-
temperature distributions shown in figure 7(b) did not provide a com-
pletely ice-free boot surface for any of the boots investigated in the
icing condition listed.

    Several curves showing typical variations of measured local surface
temperatures with time are presented in figure 8. The time-temperature
curves were obtained with the boots operating in an icing condition iden-
tical to that presented in figure 7. The curves are presented for var-
ious points on the surface of the boots and represent a portion of the
data from which the surface-temperature-distribution curves of figure 7
were obtained. The values of s/c listed correspond to the approximate
center of the most forward segments, upper and lower surfaces, of the
three boots. A comparison of figures 8(a), (b), and (c) shows that the
peak surface temperatures measured on the most forward segments of the
upper surface of the boots are lowered approximately 10° F by the pres-
ence of an icing cloud. This relatively small drop in surface tempera-
ture indicates the relatively small amount of impingement and runback
occurring over a large portion of the upper surface at an angle of

attack of 2°. Comparison with figures 8(d), (e), and (f) shows that the
temperature drop experienced on the lower surface of the boots is about
2.0 to 3.5 times as great as those measured on the upper surface for
the values of s/c shown. The irregularities and breaks noted in fig-
ures 8(d), (e), and (f) occurred at random intervals and are associated
with slow or incomplete shedding of ice, sliding of ice back over the
thermocouple junctions, and freezing of water as the surface of the boot
falls below the freezing level. For example, the time-temperature curve
presented in figure 8(e) shows rapid changes occurring in both the heat-
ing and cooling portions of the curve. The abrupt rise in temperature
experienced at 6.5 seconds indicates a sudden removal of ice from the
surface at that time, while the break noted at 30 seconds is due to the
freezing of water on the surface of the boot.

The effect of angle of attack on the surface-temperature distribu-
tion for boot A operating in dry air and in icing is shown in figure 9.
The temperatures presented are peak values measured at the end of the
individual heat-on periods. A considerable change in surface-temperature
distribution was observed when the angle of attack was changed from 2°
to 6° in dry air, as evidenced in figure 9(a). The largest effect was
the change in the temperatures of the parting strip and forward seg-
ments on the upper and lower surfaces. The 14° F drop in parting-strip
surface temperature is due to the movement of the stagnation point to
the lower surface of the airfoil. At high angle of attack, the parting
strip has moved so that the local air velocities over it are high, which
results in higher convective heat transfer from the surface (the
parting-strip surface thermocouple was located at the stagnation point
for zero angle of attack).

In an icing condition, increasing the angle of attack from 2° to
6° had practically no effect on the temperature distribution over the
upper surface of the boot (fig. 9(b)). The temperatures measured across
the lower surface of the boot were higher for the higher angle of
attack, while the parting-strip temperature was lowered approximately
5° F by the angle-of-attack increase. For the moderate icing condition
listed, the surface-temperature distributions shown in figure 9(b)
resulted in essentially complete shedding of ice from the boot surface
at both 2° and 6° angles of attack.

The effect of free-stream velocity on the surface-temperature dis-
tribution measured for boot A in dry air and in icing is shown in fig-
ure 10. For the boot operating in dry air at an angle of 2°
(fig. 10(a)), increasing the free-stream velocity from 288 to 397 feet
per second resulted in lowered surface temperatures over the entire sur-
face of the boot. The greatest temperature decreases occurred in the
area of the parting strip and forward cycled segments. A maximum
decrease of approximately 28° F was observed on segment AL1 at an s/c
of 2.0 percent.

The variation of the surface-temperature distribution measured in icing for the two values of free-stream velocity is plotted in figure 10(b). The surface temperatures measured at the higher free-stream velocity were all lower than those measured at a free-stream velocity of 288 feet per second, with the exception of segments AU2 and AU3 (upper surface) which were relatively unaffected by the appreciable increase in velocity for the icing condition listed. The maximum decrease in surface temperature occurred on the lower surface at an s/c of approximately 3.0 percent. The surface-temperature distributions shown in figure 10(b) resulted in complete shedding of ice from the heated surface of the boot for both free-stream velocities investigated.

Boot B was used to study the effect of increasing power density (cycled areas) on measured surface-temperature distribution. The variation of surface-temperature distribution for various values of power density and heat-on time is shown in figure 11. The lower dashed curve represents the normal operating conditions for the boot (21.0 w/sq in. for cycled area, 13.0 w/sq in. for parting strip, and a heat-on time of approximately 10 sec). For an icing condition having a free-stream total temperature of 15° F, a free-stream velocity of 395 feet per second, a liquid-water content of 0.55 gram per cubic meter, and a droplet diameter of 12 microns, the normal cycle did not provide complete ice shedding from the surface. Increasing the power density from 21 to 30 watts per square inch and decreasing the heat-on time from 10.2 to 7.0 seconds, thus maintaining a constant input power of approximately 210 watt-seconds to each cycled segment, resulted in higher surface temperatures for all cycled segments, as evidenced by the middle curve presented in figure 11. This more favorable temperature distribution resulted in better shedding characteristics for the boot; however, complete shedding was not attained. Maintaining the power density of 30 watts per square inch and operating the boot at the normal heat-on time of about 10 seconds resulted in the temperature distribution represented by the upper (solid) curve of figure 11. With the boot operating at this over-design condition, complete shedding of ice was attained for each cycle. For the curves shown in figure 11, the parting strip was operated continuously at a power density of 13.0 watts per square inch. Operation at a power density of 30 watts per square inch and a heat-on time of 10 seconds for approximately 30 minutes in the icing condition listed in figure 11 had no apparent detrimental effect on the boot.

Typical variations of local surface temperature measured at a value of s/c of 8.86 percent, upper and lower surfaces, for boot B in icing are shown in figure 12 for several values of power density and heat-on time. The temperatures were measured at the approximate center of segments BU2 and BL2 and in an icing condition identical to that presented in figure 11. In figure 12(b) it can be noted that, for a power density

of approximately 30 watts per square inch, the temperature measured at
the center of segment BL2 rose to approximately 32° F even before heat
was applied to that segment. This rise was probably due to runback
resulting from the application of heat to segment BL1 forward of BL2.

A limited number of temperature measurements made on the aluminum
skin beneath the boots showed that the fluctuations of aluminum skin
temperatures with time were only of the order of 10° F during the time
interval $\left(1\frac{2}{3} \text{ min}\right)$ required for one complete cycle. These rather small
fluctuations in skin temperature result from the cycle ratio and heat-on
time employed and from the thermal insulating properties of the boots.
For a cycle ratio of 10 and a heat-on period of 10 seconds, the residual
heat in the boots is not dissipated into the aluminum skin during the
short heat-off period of $1\frac{1}{2}$ minutes. Measurements on the upper surface
of the airfoil model beneath boot B showed the maximum aluminum skin tem-
peratures to vary almost linearly with s/c from a maximum of 85° F
measured beneath the parting strip to a value of 47° F beneath segment BU3
for the following operating conditions: normal cycle, dry air, design
power density, free-stream total temperature of 15° F, free-stream velocity
of 398 feet per second, and angle of attack of 2°. Skin temperatures
measured at isolated points beneath the other two boots indicate that the
aforementioned values of skin temperature and temperature fluctuation are
typical for all boots investigated.

General De-Icing and Runback Characteristics

The icing and runback characteristics of boots A, B, and C operating
with the local surface temperatures and the temperature distributions
presented in figures 7 and 8 are shown in figure 13. The photographs
show the appearance of the upper surface of the boots after 14 and
22 minutes in the following icing conditions: free-stream total tem-
perature, 15° F; free-stream velocity, 396 feet per second; liquid-water
content, 0.57 gram per cubic meter; and angle of attack, 2°. It is
apparent that, for these icing conditions, none of the boots provide
complete shedding of ice from the surface for operation at design power
densities and heat-on time. For longer periods of time in the abovemen-
tioned icing condition, the amount of ice adhering to boots B and C
remained relatively unchanged, while the amount of ice adhering to
boot A increased slightly, which indicated that boot A provides only
marginal icing protection for the condition listed. The photographs
showing boots A and B indicate the amount of residual ice after the
application of heat to segments AU3 and BU3. The photograph of boot C
was taken the instant heat was discontinued on segment CU2 and applied
to segment CU3. The ice adhering to segments CU3 and CU4 shed clean
when heat was applied to these segments.

2786

The photographs shown in figure 13 are typical of the comparative de-icing characteristics of the boots operating in similar icing conditions. In general, for the icing conditions investigated, no appreciable differences in the performance characteristics of boots B and C were observed. Boot B had a fine-textured clothlike surface as compared with the smoother surface of boot C, but this slight difference in surface roughness had little or no effect on ice removal. As evidenced in figure 13, the amount of icing protection afforded by boot A was slightly lower than that of the other two boots; and, hence, the boot provides marginal protection at a slightly higher value of free-stream temperature than does boot B or C, other conditions being equal. In general, for a free-stream velocity of about 395 feet per second, an angle of attack of 2°, and a liquid-water content of 0.5 to 0.6 gram per cubic meter, the range of free-stream total temperatures at which the icing protection afforded by the various boots became marginal was from 12° to 15° F. The slightly lower performance characteristics observed for boot A are attributable to the internal construction of the boot. The presence of rather large bus bars (which act as heat sinks), small unheated areas between all cycled segments, and heater wires running parallel to the airflow at 1/8-inch spacing all contribute to local cold spots from which ice fails to shed during heat-on time. The ice adhering between segments of boot A (fig. 13) is typical of the icing characteristics of the boot. In some cases the ice adhering between segments formed ahead of and behind the small unheated areas between segments to a length of 1 inch or more without adhering to the heated areas. In figure 13(a) it can be noted that considerable ice has formed on the unheated area between the parting strip and the forward cycled segment.

A comparison of figures 13(a), (b), and (c) shows that the runback pattern obtained for the boots in the icing condition listed is quite similar, with no runback occurring on the aluminum skin behind the boot scarf. The runback is a smooth clear ice formation not exceeding 1/8 inch in thickness on the upper surface.

At values of free-stream total temperature of approximately 15° F and less and for velocities of approximately 395 feet per second, the runback was limited essentially to the scarf areas for an angle of attack of 2° and liquid-water contents to 0.6 gram per cubic meter. However, since the boots did not maintain the surface clear of ice at these lower temperatures, the detrimental effect of the small amount of runback is probably slight in comparison with that due to ice accretions observed on the upper surface near the leading edge.

The runback pattern obtained on boots A and B after 56 minutes in icing at a free-stream total temperature of 20° F and a liquid-water content of 0.54 gram per cubic meter is shown in figure 14 for a free-stream velocity of 396 feet per second and a 2° angle of attack. The thickness

of the runback ice shown in figure 14 was about the same for both boots, measuring approximately 1/8 inch thick on the upper surface and 1/4 to 5/16 inch thick on the lower surface. With the boots operating at design power densities and a heat-on time of 11.0 seconds, the heated portion of the boots shed completely clear of ice on each cycle. In general, at the higher tunnel air temperatures and for a free-stream velocity of approximately 395 feet per second, the runback increased in thickness and chordwise extent because of the longer time at which the boot surface remained above the freezing level after a heat-on period.

The runback pattern obtained on boots A and B after 32 minutes of operation in icing at the lowest value of free-stream velocity investigated (288 ft/sec) is presented in figure 15. The runback pattern was obtained in an icing condition having a free-stream total temperature of 20° F, a liquid-water content of 0.66 gram per cubic meter, and a droplet size of 14 microns. The boots were operated at design power density, a heat-on time of 10.0 seconds, and an angle of attack of 2°. The runback pattern and nature of the ice formations observed on the upper and lower surfaces of both boots were found to be very similar. The runback ice was rather clear and smooth. On the lower surface, the runback ice formed a solid sheet approximately 1/4 inch thick for a distance of approximately 3 to 4 inches behind the heated area before changing into a rivulet-like formation which extended back an additional 4 to 8 inches. On the upper surface of the airfoil, the runback ice was approximately 1/8 inch thick with thin rivulet-type ice formations extending as far back as 12 inches behind the heated area.

As can be noted from a comparison of figures 14 and 15, the effect of decreasing speed in a given icing condition is an increase in chordwise extent of runback icing, with a corresponding decrease in runback ice thickness. Although figures 14 and 15 present runback patterns obtained in different icing conditions, the conditions are not so different as to preclude a comparison or an effect due to changes in free-stream velocity.

The runback pattern obtained on the upper and lower surfaces of boots A and C after 32 minutes of operation in an icing condition similar to that presented in figure 14 is shown in figure 16. The runback pattern was obtained in the following icing condition: free-stream total temperature, 20° F; liquid-water content, 0.55 gram per cubic meter; droplet size, 14 microns. The boots were operated at design power densities, a heat-on time of 10.3 seconds, and an angle of attack of 2°. For boot A, runback ice occurred on the aluminum skin behind the boot trailing edge; whereas, for boot C, the runback ice is confined to the scarf area. This apparent difference in runback pattern is probably due to the difference in design of the scarf area of the two boots. The scarf of boot A tapers from 1/8-inch thickness just behind the heated

area to almost a feather edge at the trailing edge of the boot. Boots A
and B are designed to be mounted onto the basic airfoil, whereas boot C
is designed so that, when mounted on the airplane, the outer surface of
the boot is flush with the basic airfoil contour. For this investiga-
tion, boot C was cemented onto the leading edge of the airfoil model,
and, hence, a sharp step-off of 1/8 inch existed at the trailing edge
of the boot. If this difference in trailing-edge design did not exist,
it is probable that the runback obtained on boot C would be very similar
to that obtained for the other two boots.

In an icing condition for which the free-stream total temperature
was 20° F, the free-stream velocity 395 feet per second, and the angle of
attack 2°, no secondary buildup of runback ice was observed for opera-
tion in clouds composed of droplets whose diameters were less than
15 microns. When larger droplet diameters were employed, direct impinge-
ment occurred on the runback ice, and the typical mushroom-ice forma-
tions associated with higher-temperature icing were observed on the
lower surface behind the heated portion of the boots. At times the
mushroom ice attained a height of 2 to $2\frac{1}{2}$ inches before being removed
by the aerodynamic forces. For a free-stream total temperature of 25° F
and high liquid-water contents, the effective parting strip became very
wide, extending at times beyond the center of the forward segments. In
addition, in some instances the entire upper or lower surface of the
boots was observed to be above the freezing temperature for a short
interval of time. During this interval, runback, of course, occurred
over the entire surface. Because of the nature of the cooling curves
and the manner in which the boots were cycled, the surface temperature
of the forward segments did not cool to 32° F before the application of
power raised the temperature of the rearmost segments above the freezing
value. For example, for boots A and B operating at 10-seconds heat-on
time, the surface temperature of segment U3 will exceed 32° F approxi-
mately 12 seconds after heat is discontinued on segment U1.

Boots A and B were investigated in an icing condition having a free-
stream total temperature of 0° F, a free-stream velocity of 400 feet per
second, and a liquid-water content of 0.56 gram per cubic meter. Their
icing characteristics in this condition at normal power densities but at
approximately 11-seconds heat-on time are shown in figure 17. Photo-
graphs were taken after 6 and 22 minutes in the icing condition. Both
boots began icing on the forward cycled segments, upper and lower sur-
faces, from the beginning of the icing exposure. After 15 minutes of
icing, the parting strip of each boot was narrowed by approximately
1/2 inch because of the building forward of ice from the cycled area.
The parting strip of each boot was completely bridged with ice after
20 minutes in the icing condition. In order to determine the de-icing
ability of the boots after leaving an icing condition, the tunnel cloud

2786

was discontinued after 22 minutes while boot power remained on. After 9 minutes of cyclic operation in clear air, no ice was removed from the surface of either boot.

As a result of the icing investigation, it was found that the forward cycled segments, upper and lower surfaces, were the most critical areas for the three boots investigated. Bridging of the parting strip occurred at the more severe icing conditions included in the investigation. In some cases, parting-strip surface temperatures in excess of 75° F were recorded without effecting removal of the ice cap. Although considerable melting occurred beneath the ice cap and the resulting water melted holes through portions of the cap, the inability of the forward cycled segments to melt the bond prevented ice removal.

SUMMARY OF RESULTS

The following results were obtained from an icing investigation of three production samples of electric, cyclic de-icing boots.

1. The forward cycled segments, upper and lower surfaces, of all three boots were the most critical areas for the icing conditions investigated.

2. Unheated areas as small as 1/8 inch wide occurring in the heated surface of an external, rubber-clad, electric, cyclic de-icing boot contributed to local cold spots on which ice forms.

3. The runback characteristics of the three boots were similar.

4. The performance characteristics of two of the three boots were very similar. The icing protection afforded by the boot having small unheated areas existing between segments was slightly less than that of the other two boots.

5. For icing conditions investigated at free-stream total temperature of 15° F and less, the detrimental effect of the small amount of runback ice observed is probably small in comparison with the effect of ice adhering to the surface of the boot just aft of the parting strip because of incomplete shedding.

6. For a free-stream velocity of 395 feet per second and an angle of attack of 2°, the range of free-stream total temperatures at which the icing protection afforded by the various boots became marginal was from 12° to 15° F for the values of liquid-water content included in the investigation.

Lewis Flight Propulsion Laboratory
    National Advisory Committee for Aeronautics
        Cleveland, Ohio

REFERENCES

1. Gelder, Thomas F., Lewis, James P., and Koutz, Stanley L.: Icing
   Protection for a Turbojet Transport Airplane: Heating Requirements,
   Methods of Protection, and Performance Penalties. NACA TN 2866,
   1953.

2. Lewis, James P., and Bowden, Dean T.: Preliminary Investigation of
   Cyclic De-Icing of an Airfoil Using an External Electric Heater.
   NACA RM E51J30, 1952.

3. Gray, V. H., Bowden, D. T., and von Glahn, U.: Preliminary Results
   of Cyclical De-Icing of a Gas-Heated Airfoil. NACA RM E51J29, 1952.

2786

2786

Figure 1. - Installation of airfoil model in test section of icing research tunnel.
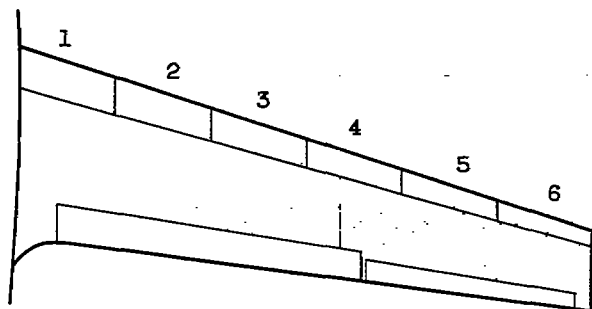
(a) Spanwise shedding.

Area
1
2
3
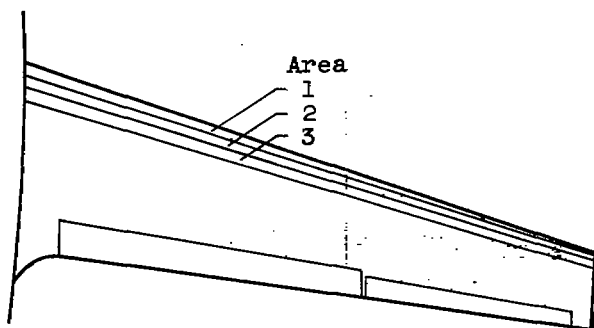
(b) Chordwise shedding.

Figure 2. - Schematic drawing of de-icing-
boot installation showing spanwise and
chordwise shedding.

AU3
BU3
AU2
BU2
AU1
BU1
AO
BO
AL1
BL1
AL2
BL2
AL3
BL3
Upper surface

CU4
CU3
CU2
CU1
CO
CL1
CL2
CL3
CL4
Upper surface
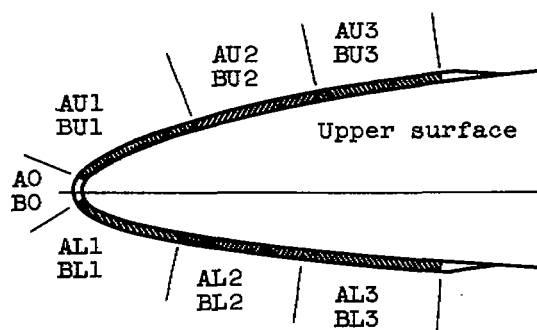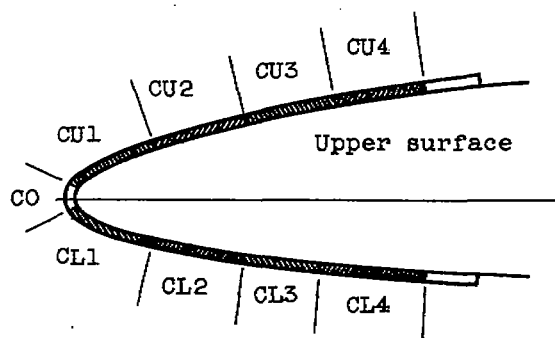
(a) Boots A and B.   (b) Boot C.

Figure 3. - Segment notation for de-icing boots used in investigation.

2786

CV-3
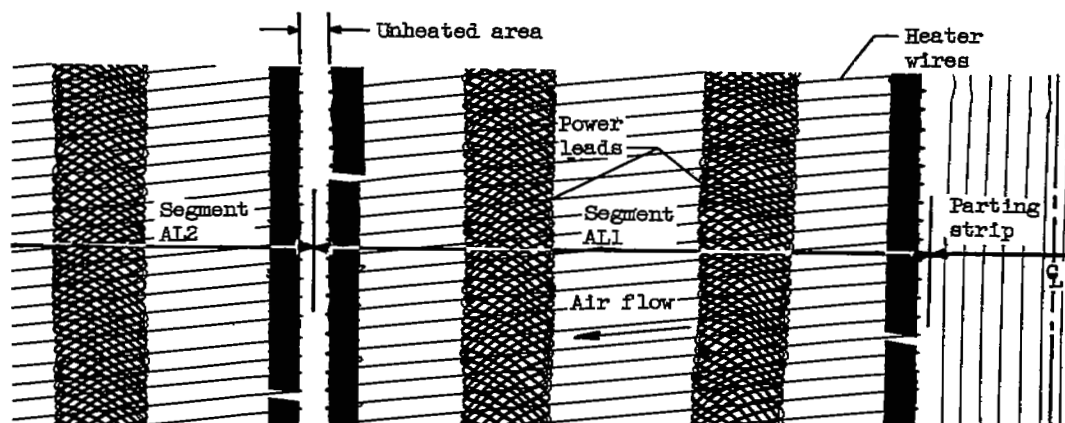
(a) Boot A.
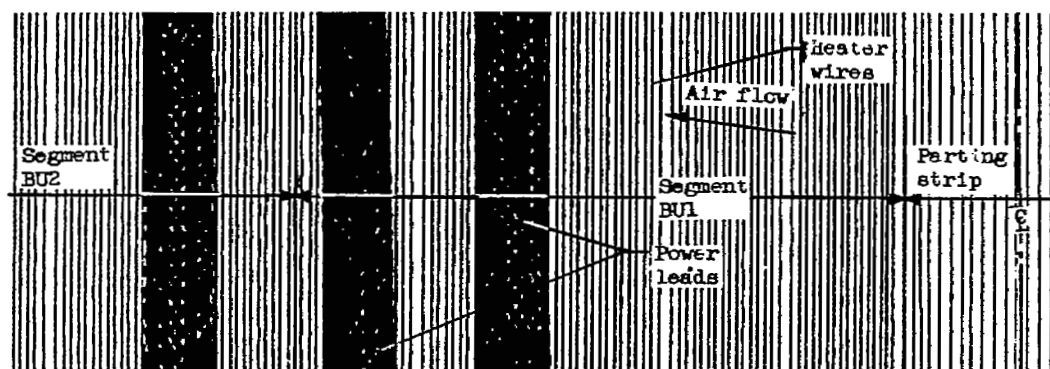
(b) Boot B.
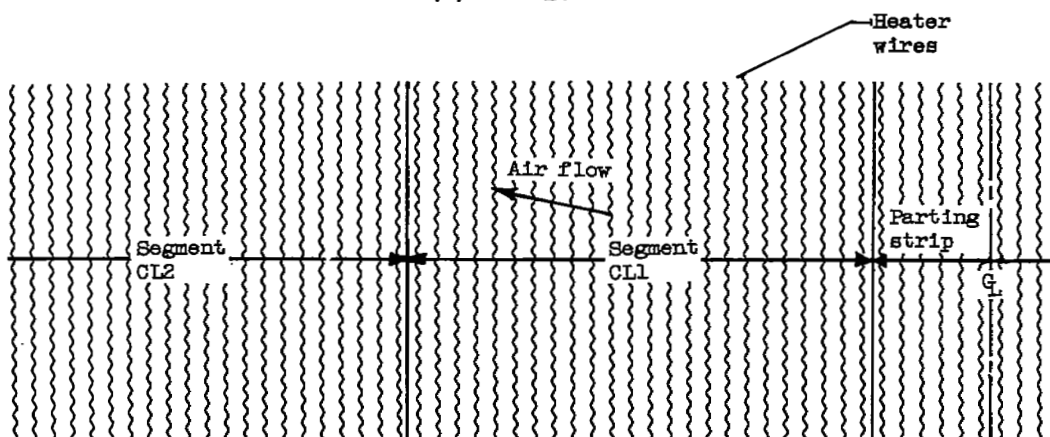
(c) Boot C.
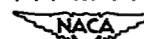
Figure 4. - Internal construction of various boots used in investigation.

C-31728
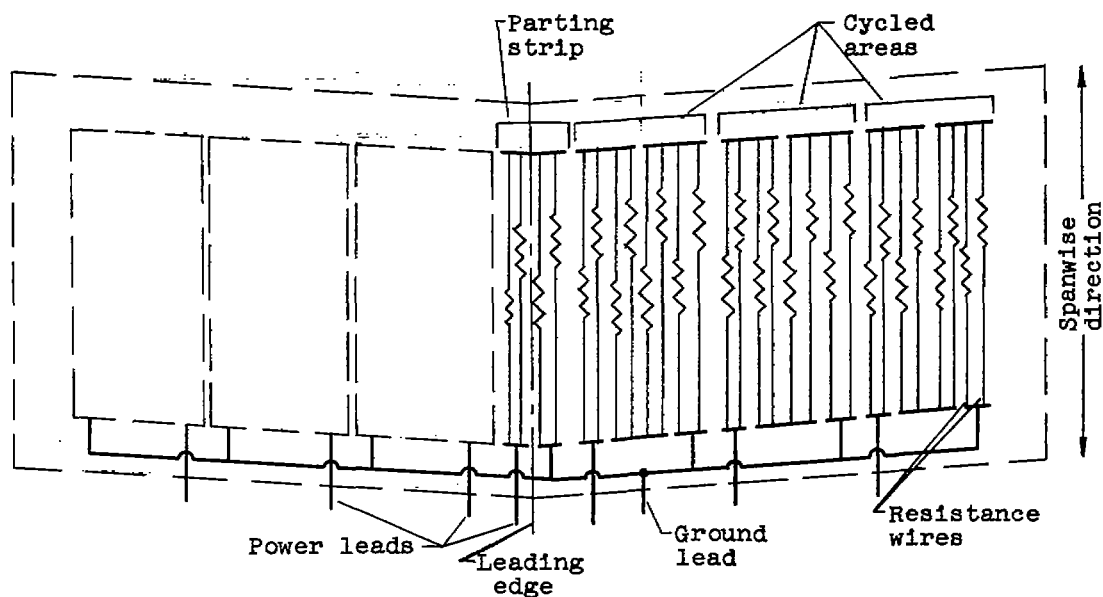
Figure 5. - Schematic diagram showing internal circuitry of boots.
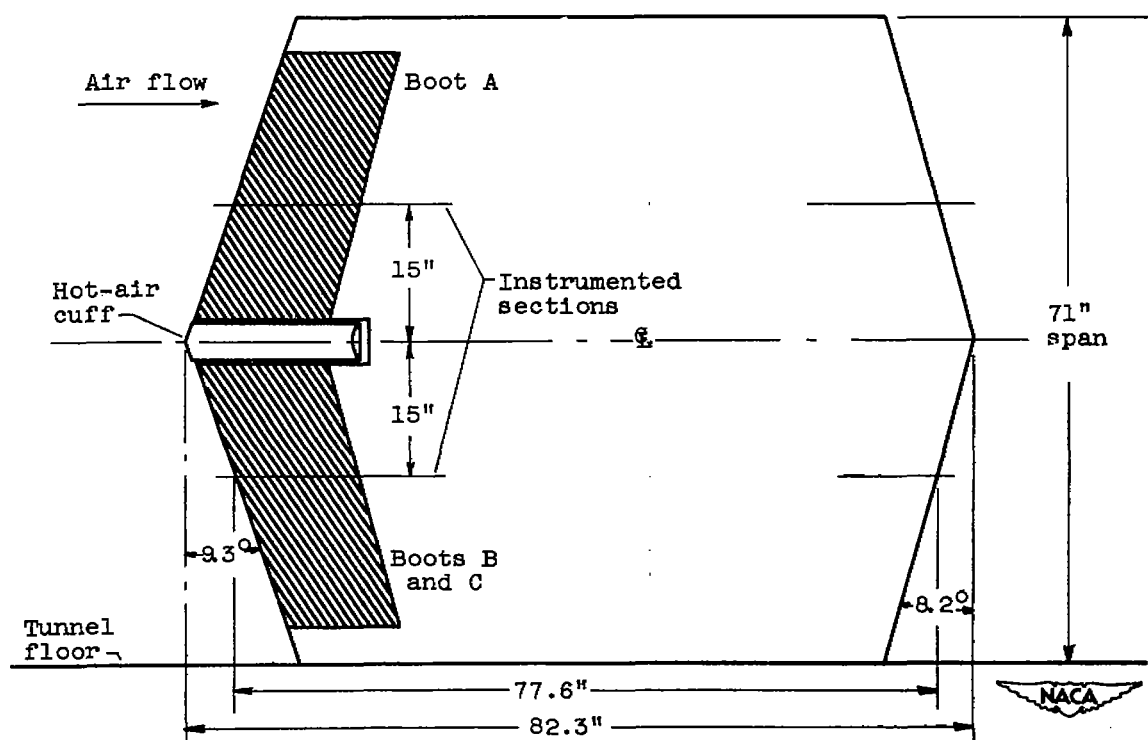
Figure 6. - Airfoil model employed in investigation.
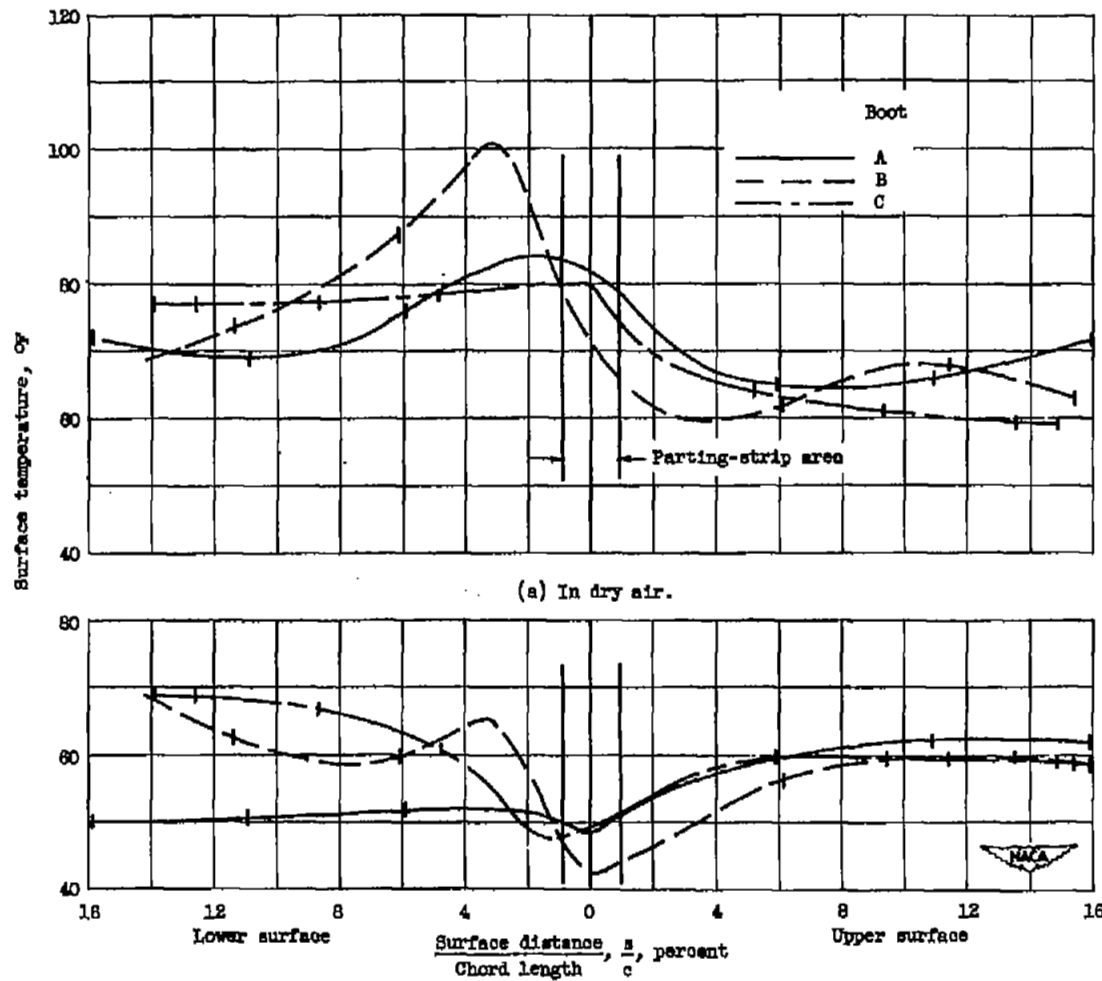
(a) In dry air.

(b) In icing. Liquid-water content, 0.57 gram per cubic meter; droplet diameter, 12 microns.

Figure 7. - Variation of surface-temperature distribution for boots A, B, and C measured in dry air and in icing. Free-stream total temperature, 15° F; free-stream velocity, 396 feet per second; angle of attack, 2°; heat-on time, 10.2 seconds; cycle ratio, 10.

(a) Boot segment AU1. Surface distance/chord length, 3.63 percent.

(b) Boot segment BU1. Surface distance/chord length, 3.54 percent.

(c) Boot segment CU1. Surface distance/chord length, 3.07 percent.
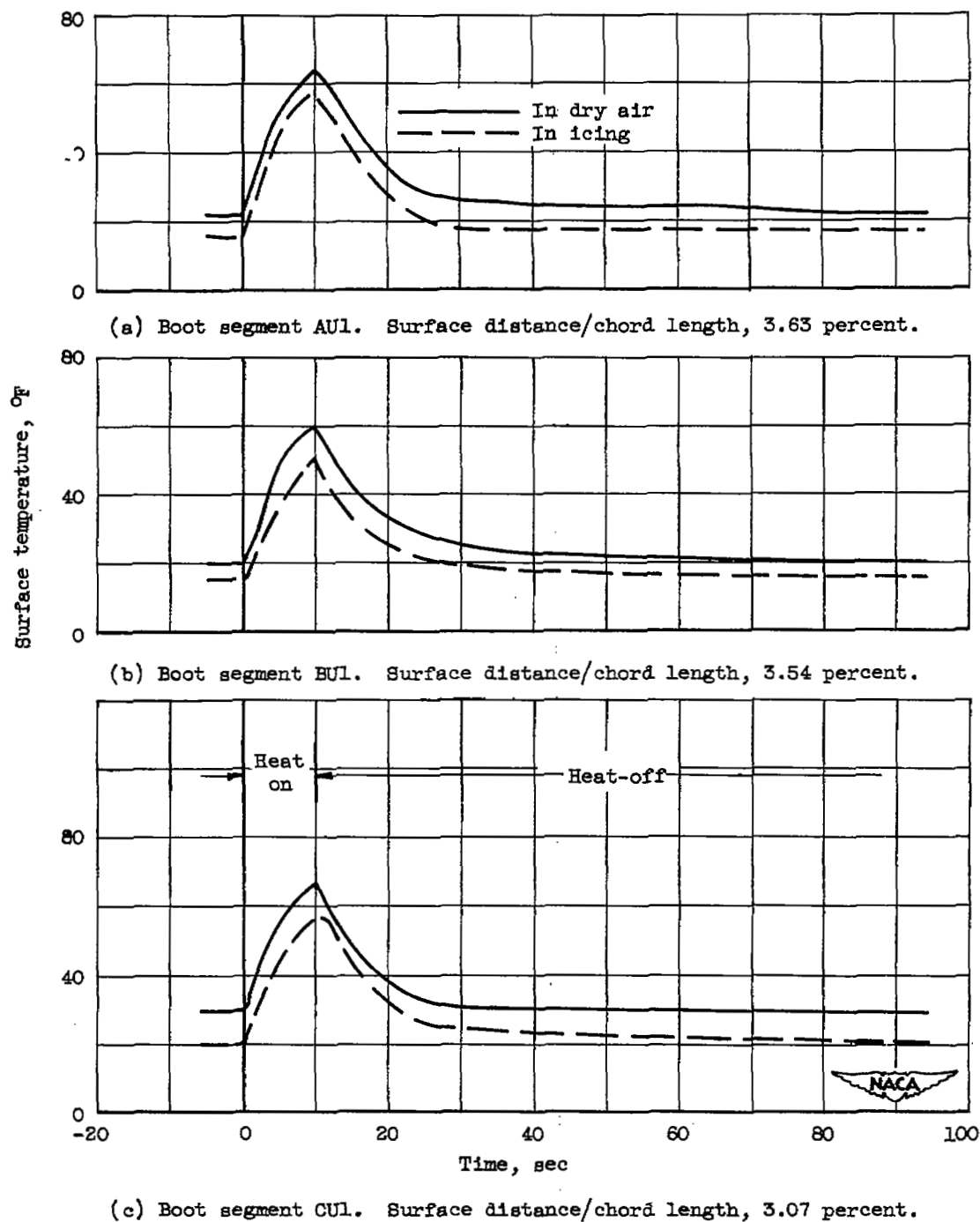
Figure 8. - Typical variation of local surface temperature, upper and lower surfaces, measured in dry air and in icing for three boots. Free-stream total temperature, 15° F; free-stream velocity, 396 feet per second; liquid-water content, 0.57 gram per cubic meter; droplet diameter, 12 microns; angle of attack, 2°; heat-on time, 10.2 seconds; cycle ratio, 10.
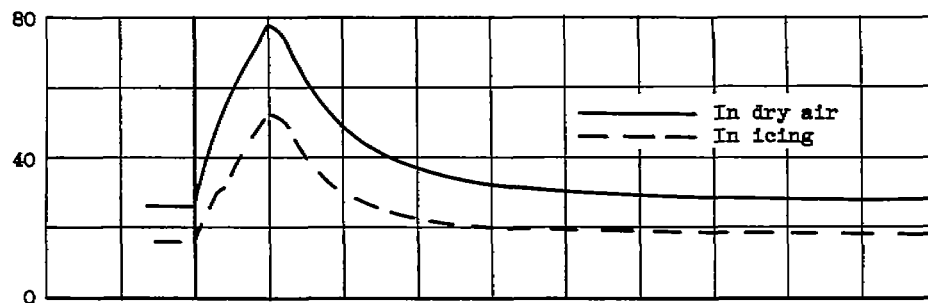
(d) Boot segment AL1. Surface distance/chord length, 3.63 percent.
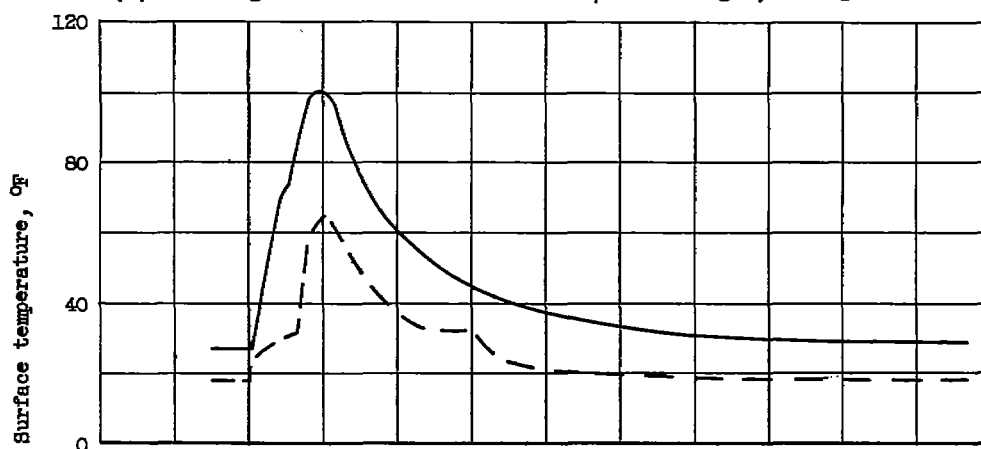
(e) Boot segment HL1. Surface distance/chord length, 3.54 percent.
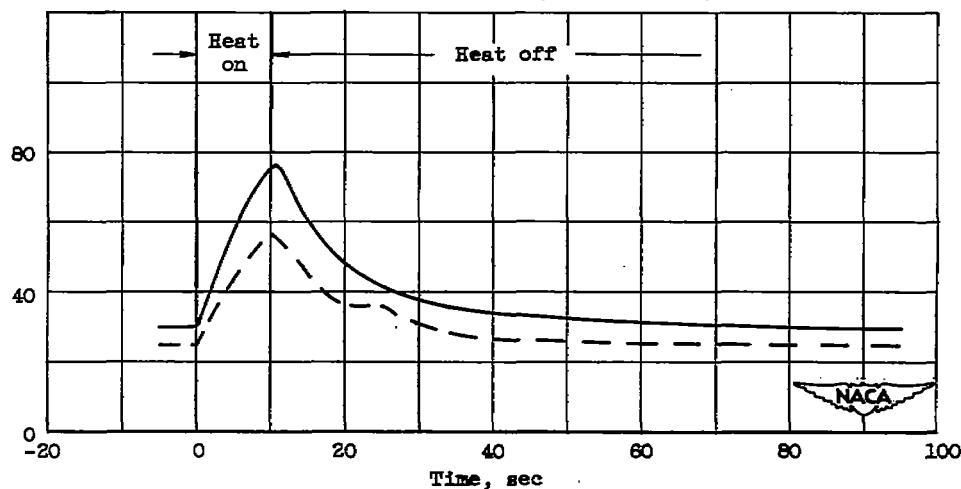
(f) Boot segment CL1. Surface distance/chord length, 2.92 percent.

Figure 8. - Concluded. Typical variation of local surface temperature,
    upper and lower surfaces, measured in dry air and in icing for three
    boots. Free-stream total temperature, 15° F; free-stream velocity,
    396 feet per second; liquid-water content, 0.57 gram per cubic meter;
    droplet diameter, 12 microns; angle of attack, 2°; heat-on time, 10.2
    seconds; cycle ratio, 10.

(a) In dry air.

(b) In icing. Droplet diameter, 12 microns.
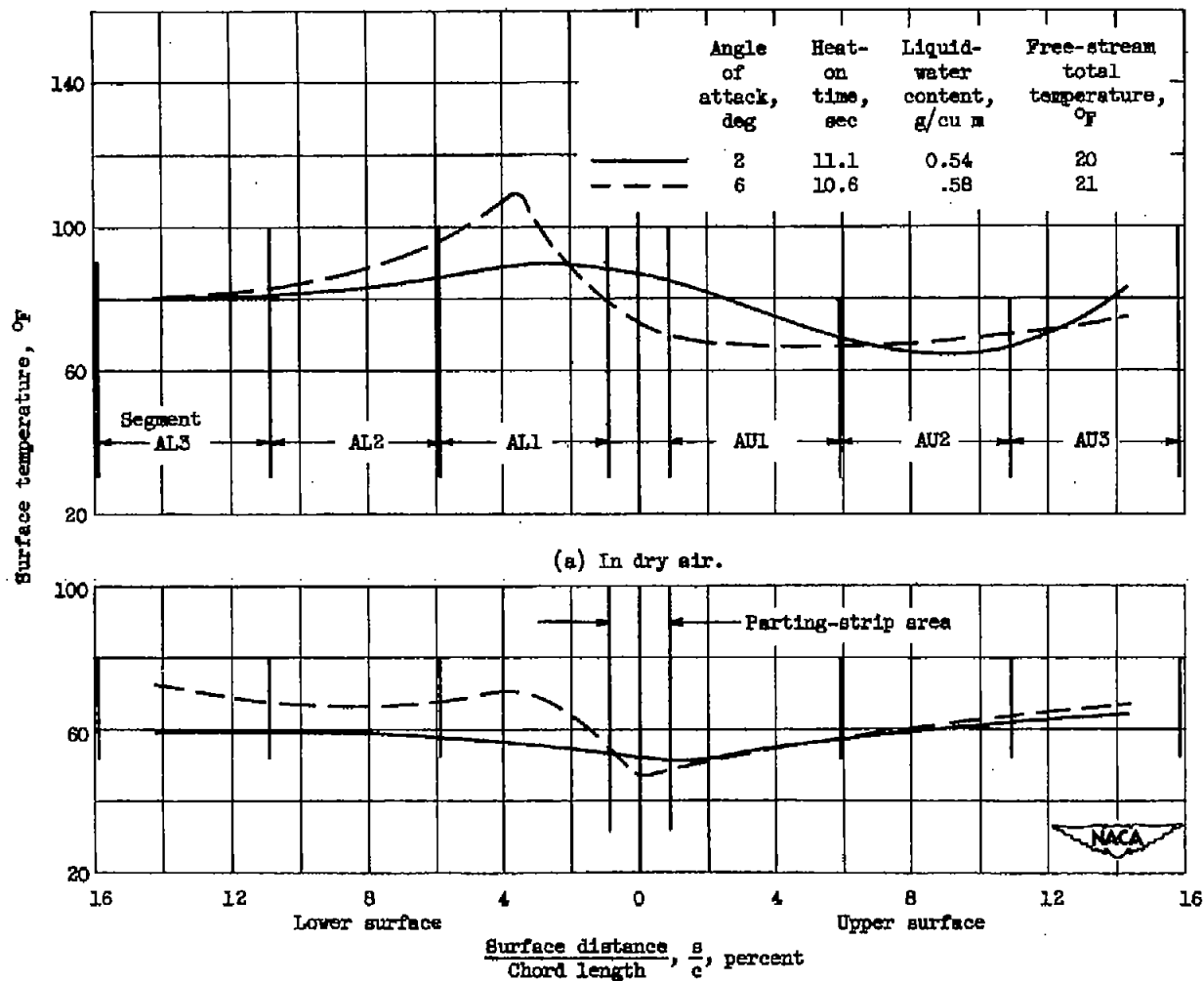
Figure 9. - Effect of angle of attack on surface-temperature distribution in dry air and in icing. Boot A; free-stream velocity, 394 feet per second.
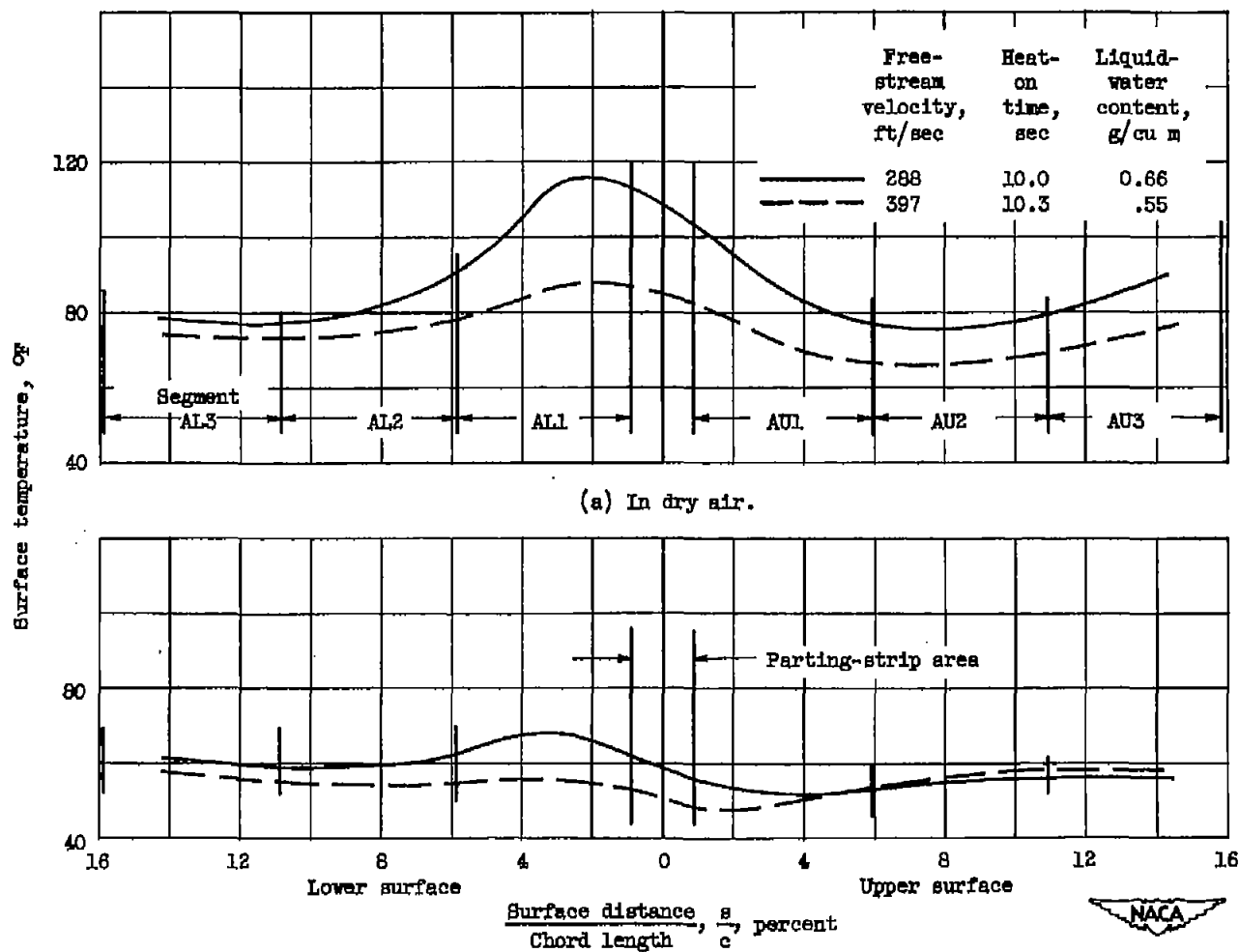
Figure 10. - Variation of surface-temperature distribution in dry air and in icing for two free-stream velocities. Boot A; free-stream total temperature, 20° F; angle of attack; 2°.
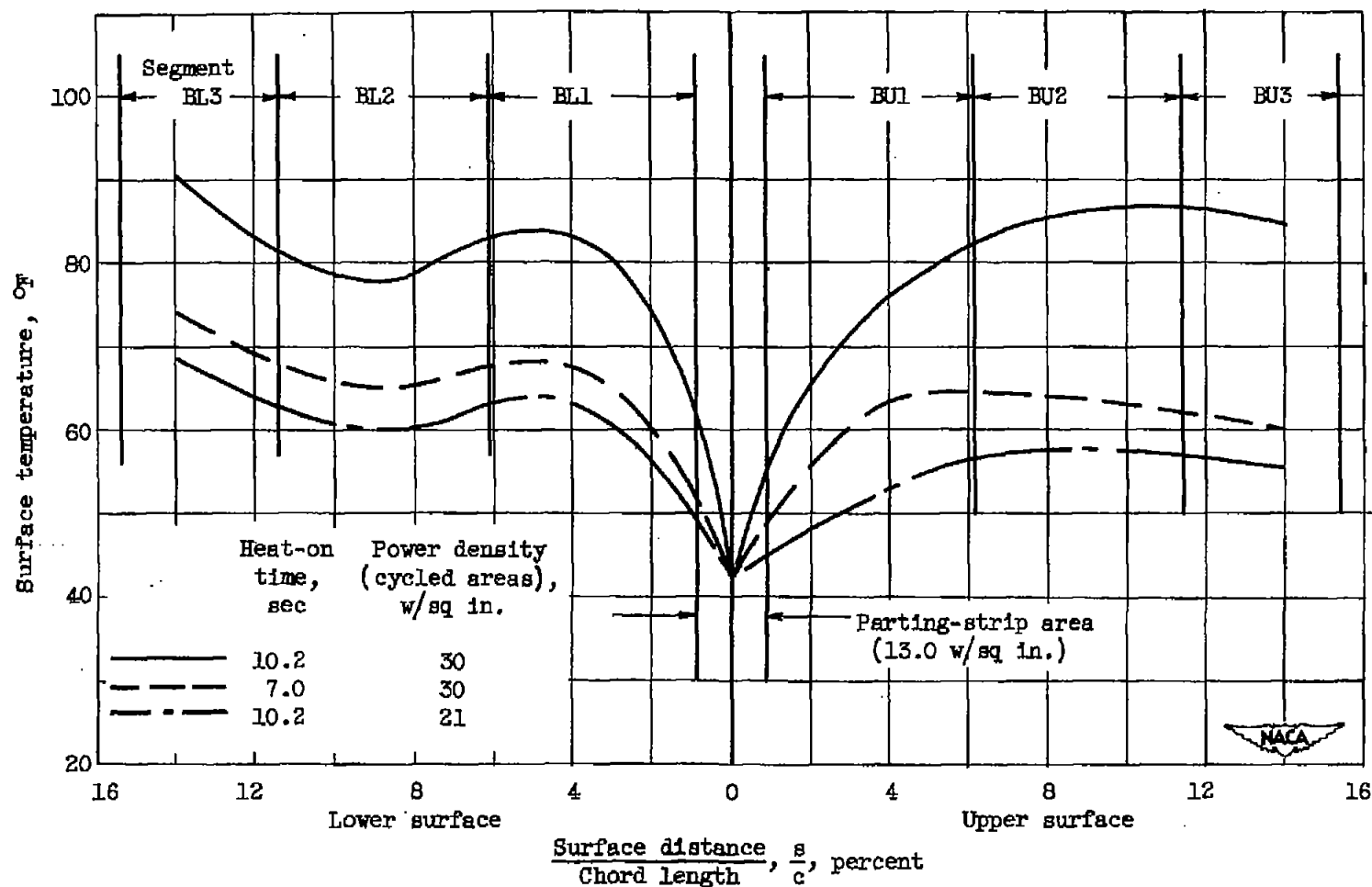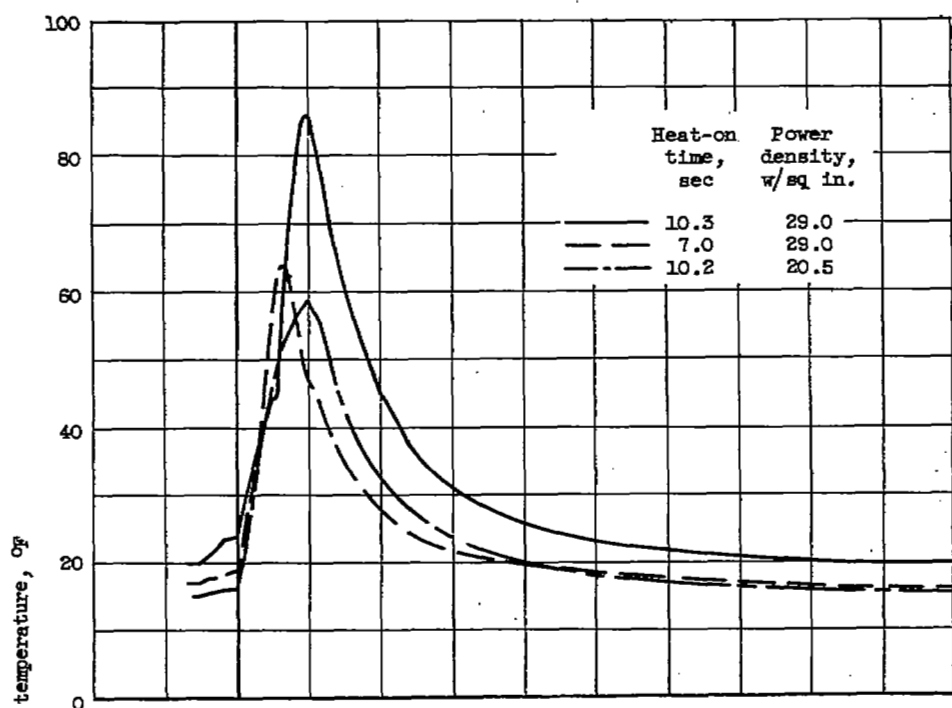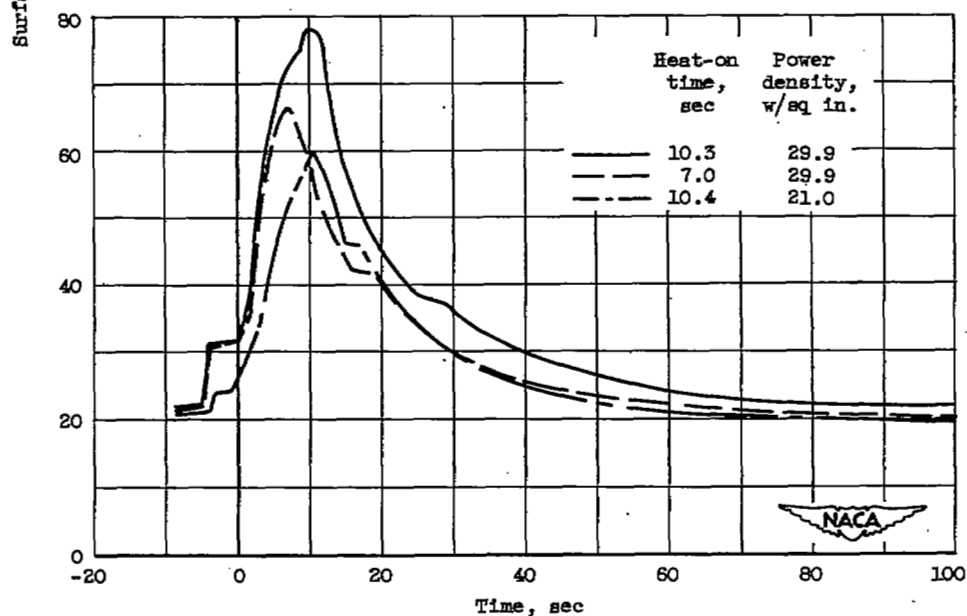
(a) In dry air.

(b) In icing. Droplet diameter, 14 microns.

Figure 11. - Variation of surface-temperature distribution measured in icing for various values of heat-on time and power density. Boot B; free-stream total temperature, 15° F; free-stream velocity, 395 feet per second; liquid-water content, 0.55 gram per cubic meter; droplet diameter, 12 microns; angle of attack, 2°.

2/86

(a) Upper surface.

(b) Lower surface.

Figure 12. - Variation of local surface temperature at s/c value of
8.86 percent, upper and lower surfaces, for various values of heat-on
time and power density. Boot B; free-stream total temperature, 15° F;
free-stream velocity, 395 feet per second; liquid-water content, 0.55
gram per cubic meter; droplet diameter, 12 microns; angle of attack, 2°.

(a) Boot A after 14 minutes in icing.

C-30304

(b) Boot B after 14 minutes in icing.

Rumback
(clear ice)

Air flow

C-30372

(c) Boot C after 22 minutes in icing.

Figure 13. - Appearance of upper surface of boots A, B, and C after several minutes in similar icing conditions. Free-stream total temperature, 15° F; free-stream velocity, 396 feet per second; liquid-water content, 0.57 gram per cubic meter; droplet diameter, 12 microns; angle of attack, 2°; heat-on time, 10.2 seconds; normal power densities.

(a) Lower surface.   (b) Upper surface.

C-30276   C-30275

Figure 14. - Runback pattern obtained on boots A and B after 56 minutes in icing. Free-stream total temperature, 20° F; free-stream velocity, 396 feet per second; liquid-water content, 0.54 gram per cubic meter; droplet diameter, 12 microns; angle of attack, 2°; heat-on time, 11 seconds; heat-off time, $1\frac{2}{3}$ minutes; normal power densities.
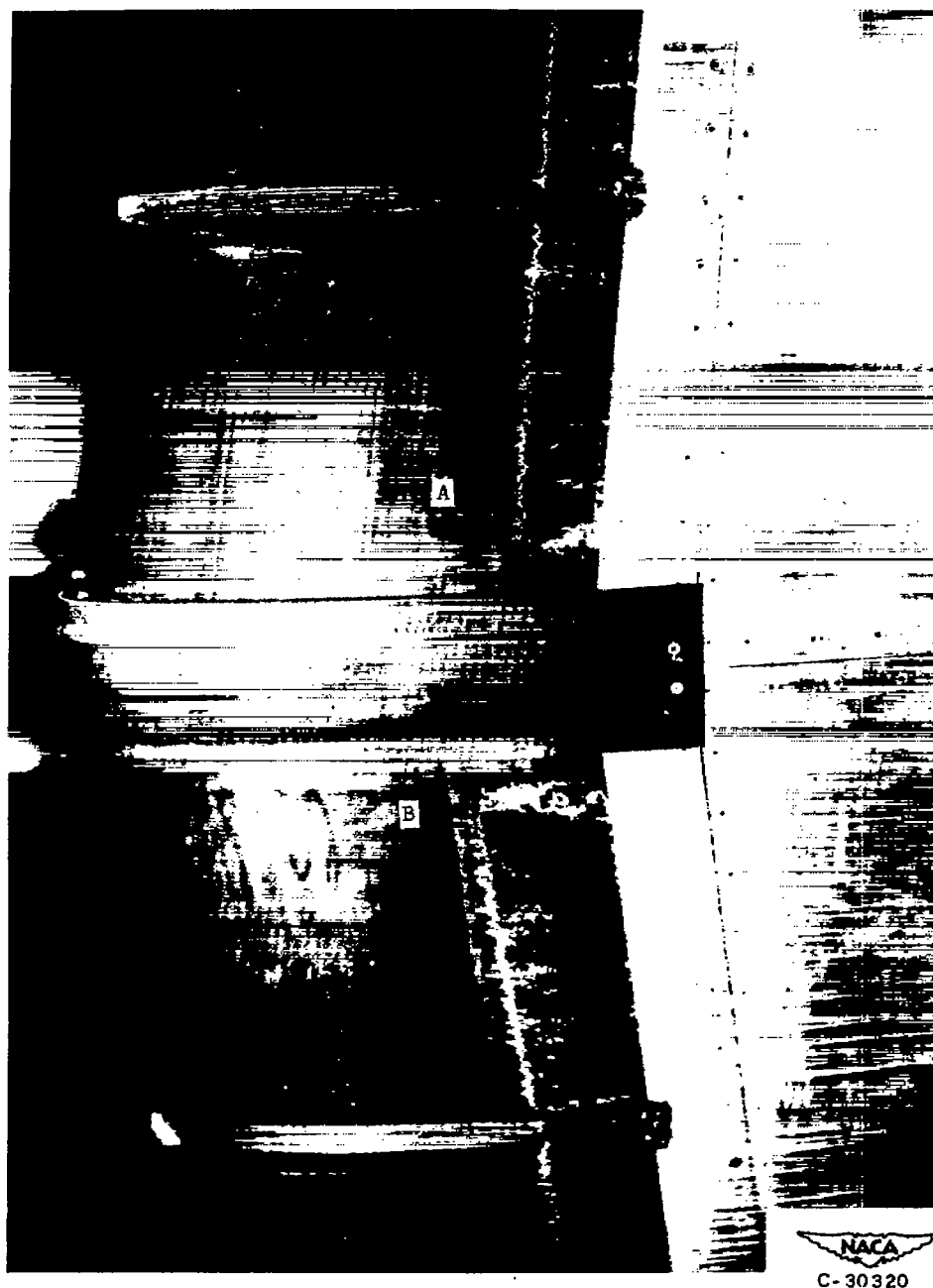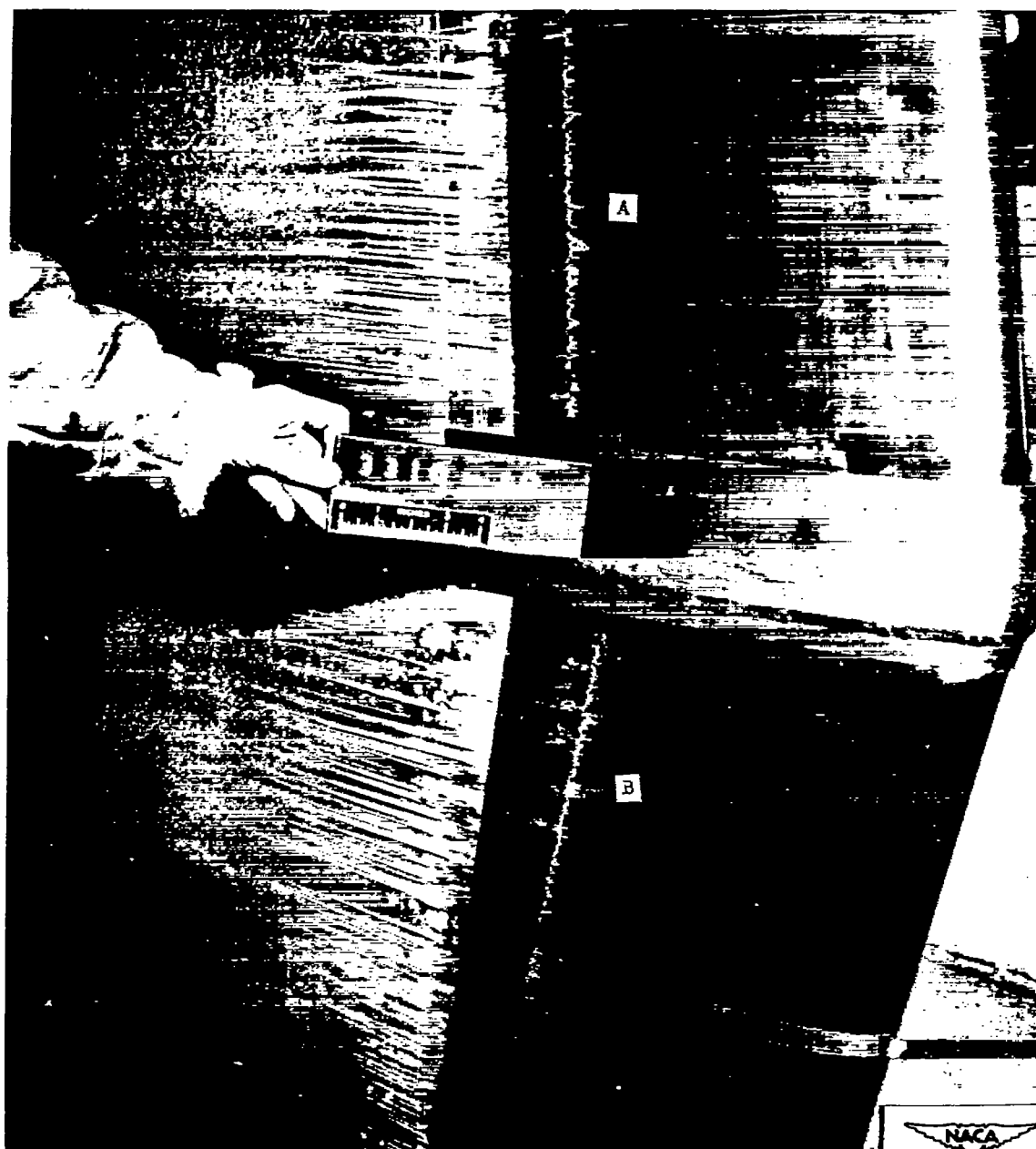
(a) Upper surface.

Figure 15. - Runback pattern obtained on boots A and B after 32 minutes in icing. Free-stream total temperature, 20° F; free-stream velocity, 288 feet per second; liquid-water content, 0.66 gram per cubic meter; droplet diameter, 14 microns; angle of attack, 2°; heat-on time, 10.0 seconds; design power densities.
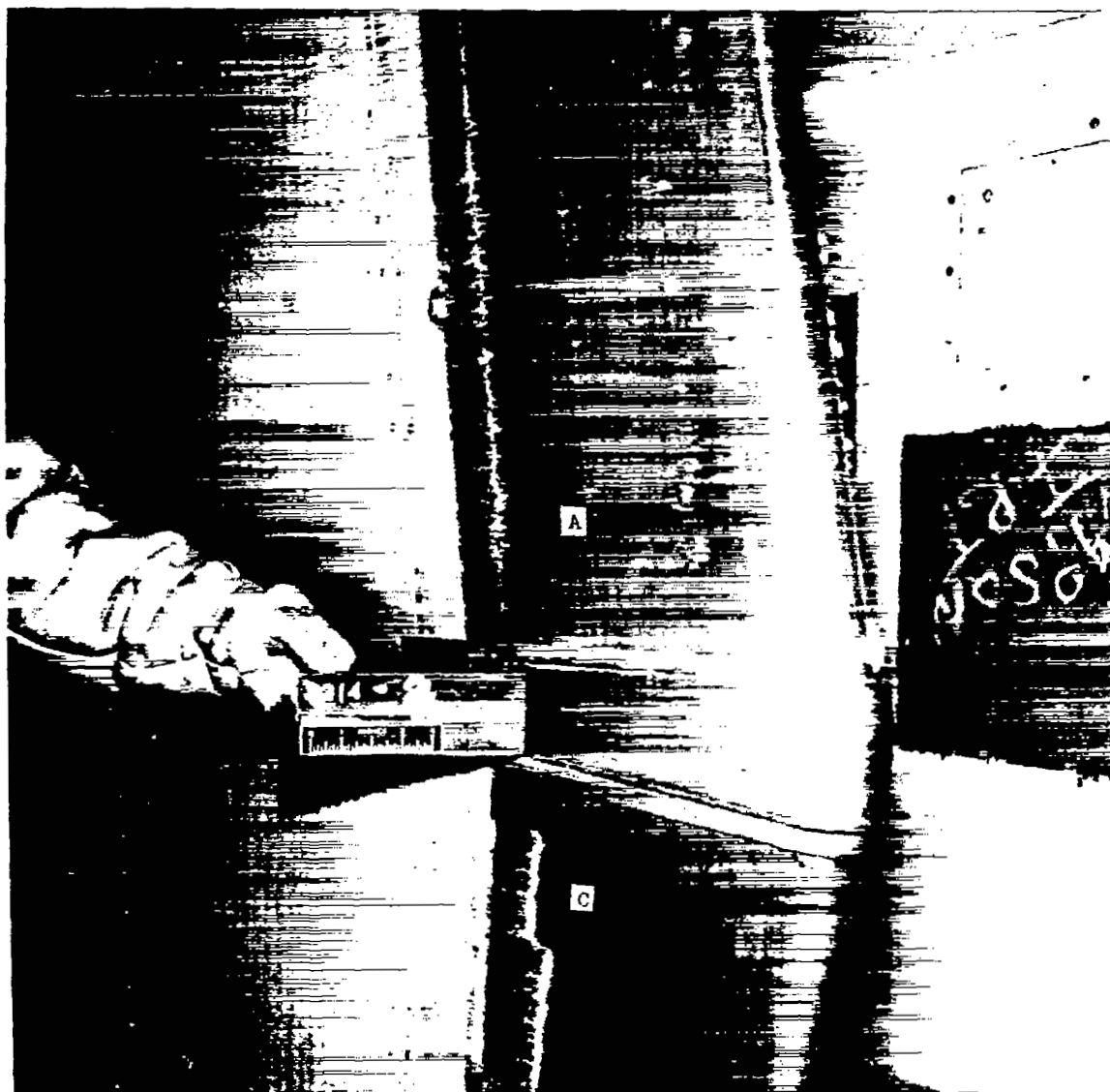
2786

(b) Lower surface.

Figure 15. - Concluded. Runback pattern obtained on boots A and B after 32 minutes in
icing. Free-stream total temperature, 20° F; free-stream velocity, 288 feet per second;
liquid-water content, 0.66 gram per cubic meter; droplet diameter, 14 microns; angle of
attack, 2°; heat-on time, 10.0 seconds; design power densities.

(a) Upper surface.

Figure 16. - Runback pattern obtained on boots A and C after 32 minutes in icing. Free-stream total temperature, 20° F; free-stream velocity, 397 feet per second; liquid-water content, 0.55 gram per cubic meter; droplet diameter, 14 microns; angle of attack, 2°; heat-on time, 10.3 seconds; design power densities.
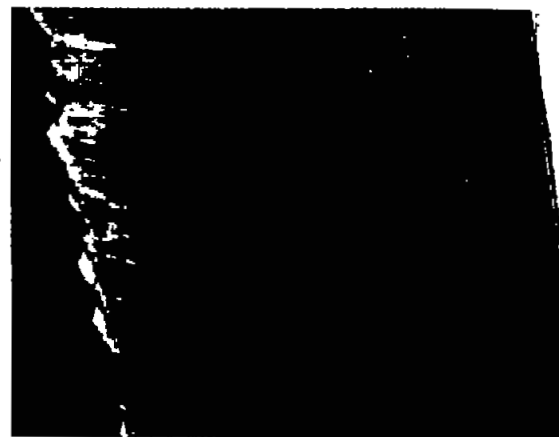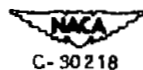
2786

(b) Lower surface.

Figure 16. - Concluded. Runback pattern obtained on boots A and C after 32 minutes in
 icing. Free-stream total temperature, 20° F; free-stream velocity, 397 feet per second;
 liquid-water content, 0.55 gram per cubic meter; droplet diameter, 14 microns; angle of
 attack, 2°; heat-on time, 10.3 seconds; design power densities.

(a) Boot A after 6 minutes in icing.

(b) Boot B after 6 minutes in icing.

C-30218

(c) Boot A after 22 minutes in icing.

(d) Boot B after 22 minutes in icing.

C-30221

Figure 17. - Appearance of boots A and B after 6 and 22 minutes in icing. Free-stream total temperature, 0° F; free-stream velocity, 400 feet per second; liquid-water content, 0.56 gram per cubic meter; droplet diameter, 10 microns; angle of attack, 2°; heat-on time, 11 seconds; normal power densities.